Catalysis Today 147S (2009) S162–S169

Contents lists available at ScienceDirect

Catalysis Today

journal homepage: www.elsevier.com/locate/cattod

Hydrodynamics of catalyst in conical spouted beds

M.J. San José *, Sonia Alvarez, Alberto Morales, Luis B. López, Alvaro Ortiz de Salazar

Departamento de Ingeniería Química, Universidad del País Vasco, Aptdo 644, 48080 Bilbao, Spain

ARTICLE INFO

Article history:
Available online 7 August 2009

Keywords:
Spouted beds
Conical spouted beds
Operating conditions
Catalyst
Thermal treatment

ABSTRACT

The applicability of conical spouted bed reactors for the thermal catalytic treatment of wastes has been determined by means of a hydrodynamic study with catalyst solids (fine particles) in different experimental conditions. The ranges of the geometric factors of the conical contactor and of the contactor–particle system for stable operating conditions have been established at gas inlet temperature range of 25–500 °C in order to achieve the stability. The validity of the correlations already proposed for calculation of minimum spouting velocity of fine particles at room temperature has been proven at high temperature (at a range of gas inlet temperatures between 25 and 500 °C).

1. Introduction

Due to the increasing costs of fossil fuels, interest has grown in the use of renewable energy. Different methods can be followed for the use of the biomass feedstocks, as combustion, gasification and pyrolysis. Spouted bed technology is suitable for thermal treatment of wastes by combustion [1–5], gasification [6–9] and by pyrolysis [6,10–18]. Therefore, due to the ability to handle granular and fibrous solids that are sticky, of irregular texture and with a wide particle size distribution [19], and mixtures of different sizes and textures with low segregation [20–22] conical spouted beds would be adequate for using energy of biomass wastes, from the environmental point of view, by the addition of an appropriate catalyst.

In previous papers [17,19], the hydrodynamics at room temperature of coarse particles ($d_p > 1$ mm) have been studied in conical spouted beds, as well as, of fine particles ($d_p \leq 1$ mm), glass spheres and catalysts [23] for catalytic polymerizations [24]. The ranges of the geometric factors of the conical contactor and of the contactor–particle system for stable operating condition have been established in order to reach the stability. In this paper, the hydrodynamics of catalyst solids (fine particles) have been studied in conical spouted beds of different geometries (contactor angle and gas inlet diameter) and in different operating conditions (stagnant bed height, particle diameter and gas velocity) at gas inlet range of 25–500 °C.

2. Experimental

The experimental unit, Fig. 1, design at pilot plant scale consists basically of a blower that supplies a maximum air flow rate of 300 N m^3 h^{-1} at a pressure of 15 kPa. The flow rate is measured by means of two mass-flow meters in the ranges of 50–300 and 0–100 m^3 h^{-1}, with both being controlled by a computer.

The measurement of the bed pressure drop is sent to a differential pressure transducer (Siemens Teleperm), which quantifies these measurements within the 0–100% range. This transducer sends the 4–20 mA signal to a data logger (Alhborn Almeno 2290-8), which is connected to a computer, where the data are registered and processed by means of the software AMR-Control. This software also registers and processes the air velocity data, which allows for the acquisition of continuous curves of pressure drop vs. air velocity [25,26].

Three conical contactors made of poly(methyl methacrylate), Fig. 2, have been used whose dimensions are as follows: column diameter, D_c, 0.14 m; diameter of the bed base, D_i, 0.012 m; contactor angle, γ, 30, 35 and 45°; gas inlet diameter, D_o, in the range of 0.004, 0.006 and 0.010 m. The values of the stagnant bed height, H_o, used are in the range between 0.05 and 0.40 m. Operation has been carried out at the minimum spouting velocity and at velocities 20 and 30% above this value.

The solids used have been Y zeolites, silica gel and Pd catalysts supported on Al_2O_3, which corresponds basically to groups A and B of the Geldart classification [27–28] and their properties are set out in Table 1. Two fractions of each catalyst type have been separated by sieving to obtain the binary mixtures of 50 wt.% of each particle, represented by the Sauter average diameter, $\overline{d_S}$, used in the experimental systems.

In order to quantify the segregation, solid sampling has been carried out by means of a probe connected to a suction pump [21]. A distance of 20 mm has been established between sampling points. The optimum sampling duration was estimated between 3 and 5 s, as shorter times give way to errors inherent in withdrawal of small amounts of sample. Each sampling is repeated three times

* Corresponding author. Tel.: +34 94 6015362; fax: +34 94 6013500.
E-mail address: mariajose.sanjose@ehu.es (M.J. San José).

0920-5861/$ – see front matter © 2009 Elsevier B.V. All rights reserved.
doi:10.1016/j.cattod.2009.07.050

Nomenclature

Ar	Archimedes number ($gd_p^3\rho(\rho_s - \rho)/\mu^2$)
D_b, D_c, D_i, D_o	upper diameter of stagnant bed height, of the column, of the bed base and of the gas inlet, respectively (m)
d_p	particle diameter (m)
d_p^*	modulus related to particle size-density ($Ar^{1/3}$)
g	gravity (m s^{-2})
$\overline{d_S}$	Sauter average particle diameter (m)
H_c, H_o	height of the conical section of the contactor and of the stagnant bed, respectively (m)
$(Re_o)_{ms}$	Reynolds number of minimum spouting referred to D_o ($u_o\rho d_p/\mu$)
u	velocity of the gas referred to D_i (m s^{-1})
u^*	velocity modulus referred to D_b ($u^* = u[\rho^2/\Delta\rho g\mu]^{1/3}$)
X_B	weight fraction of the particles of greater diameter

Greek symbols

ϕ	particle sphericity
γ	contactor angle (°)
ρ_s	solid density (kg m^{-3})
ρ	gas density (kg m^{-3})

at each position in the bed, and the solids are returned to the contactor after each sampling.

3. Results

In order to prove the applicability of the spouting regime for treatment of catalyst in conical spouted beds, a hydrodynamic study has been carried out at a range of temperatures between 25 and 500 °C.

In order to illustrate the different regimes in beds made up of catalyst with air velocity, in Fig. 3 an outline of the evolution of particle population in the different regimes is shown for beds made up of catalyst. After the fixed bed, in Fig. 3a, by increasing gas velocity, the stable regime of spouting is reached, in Fig. 3b, the velocity corresponding to the beginning of the regime of spouting is the minimum spouting velocity.

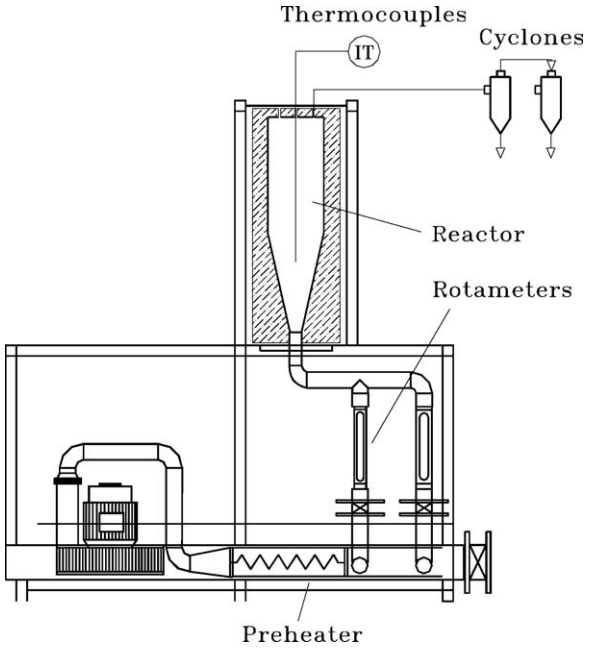

Fig. 1. Diagram of the experimental equipment.

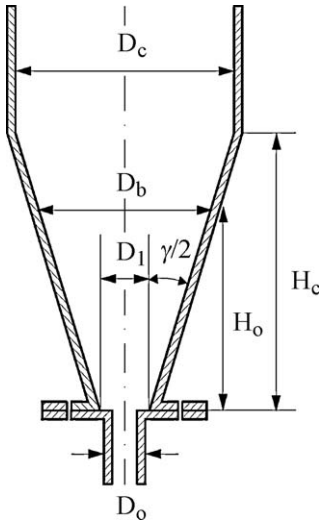

Fig. 2. Geometric factors of the contactor.

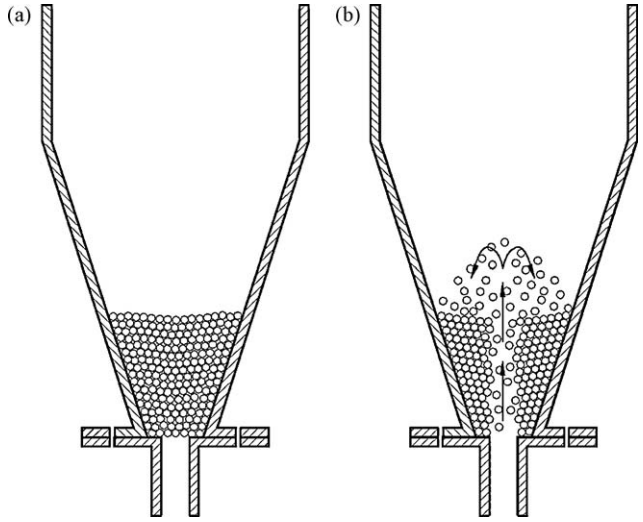

Fig. 3. Particle states in the contactor in (a) fixed bed and (b) spouted bed regime.

3.1. Pressure drop evolution with air velocity

In order to illustrate the general characteristics of pressure drop evolution in the bed with air velocity, in Fig. 4, the results for one spouted bed (contactor geometry: $\gamma = 35°$; $D_o = 0.006$ m) and for a bed consisting of binary mixtures of silica gel of Sauter average diameter $\overline{d_S}$ 0.40 mm and for different values of the stagnant bed height, are shown as an example. The evolution of pressure drop by decreasing gas flow is plotted in dotted line.

This diagram is similar to that of conical spouted bed reactor for coarse particles [14]. After the state of fixed bed, velocity becomes the value corresponding to the maximum pressure drop. After this, the pressure drop decreases sharply to the value of the stable pressure drop. As it is observed, maximum pressure drop obtained by decreasing the gas velocity is much lower than that measured by increasing the air flow, therefore the hysteresis is noticeable. In addition, the hysteresis is more pronounced in conical spouted

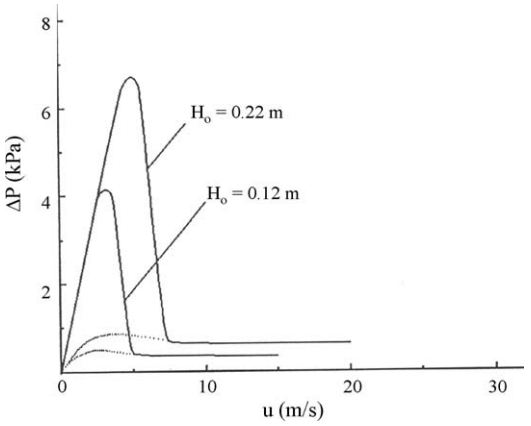

Fig. 4. Evolution of the pressure drop with air velocity for different values of the stagnant bed height. Experimental conditions: $\gamma = 35^\circ$; $D_o = 0.006$ m, silica gel of $\overline{d_S}$ 0.40 mm.

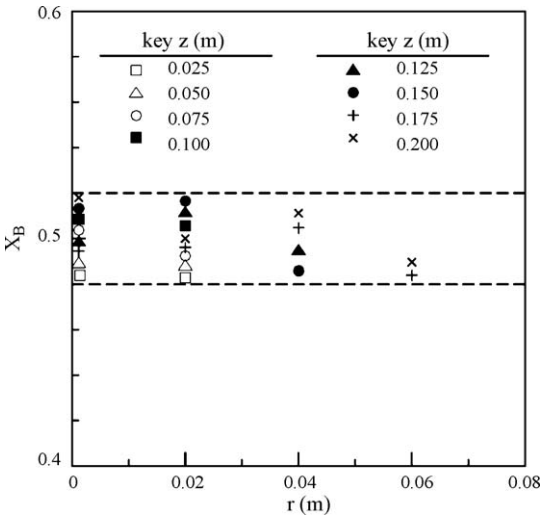

Fig. 5. Weight fraction of the particles of greater diameter at different positions of the bed. System: $\gamma = 35^\circ$, $D_o = 0.006$ m, binary mixture of silica gel of $\overline{d_S}$ 0.40 mm.

beds in beds consisting of fine particles than the observed in beds consisting of coarse particles, at the same experimental conditions [19]. The velocity corresponding to the beginning of the spouted bed regime is the minimum spouting velocity.

The experimental value of this velocity is determined from the values of pressure drop by decreasing slowly the gas flow at the point when the pressure drop levels off, because this velocity is more accurate and reproducible than the one obtained by increasing the gas flow.

3.2. Operating stability and conditions of nonsegregation

In order to carry out the hydrodynamic study, segregation of all mixtures has been studied, with the aim of delimiting those mixtures that do not have any noticeable segregation.

In Fig. 5, the weight fraction of the particles of greater diameter, X_B, at different radial and longitudinal positions of the bed has been plotted as an example of the results for a mixture without noticeable segregation (corresponding to 50 wt.% of each size of silica gel of Sauter mean diameter $\overline{d_S}$ 0.40 mm, $\gamma = 35^\circ$; $D_o = 0.006$ m). As it is observed, the bed composition is practically uniform, with values between 0.48 and 0.52 and the experimental error estimated in the measurement is ±1%. It has been proven that the other binary mixtures of Table 1 present results of nonsegregation similar to Fig. 5.

The stable operating conditions in conical spouted beds have been plotted in a classic diagram such as the proposed by Mathur and Gishler [29] for conventional spouted beds. In this diagram, the stagnant bed height, H_o, has been plotted against the gas velocity, u. The borders between the different regimes, drawn with solid lines, have been obtained theoretically and the points correspond to the experimental values, by increasing gas velocity for each stagnant bed height.

The stability diagram H_o against u for the conical contactor angle $\gamma = 35^\circ$, gas inlet diameter, $D_o = 0.04$ m, with a bed of a binary mixture of silica gel of Sauter mean diameter $\overline{d_S}$ 0.40 mm, at temperatures of 30 °C, is shown in Fig. 6.

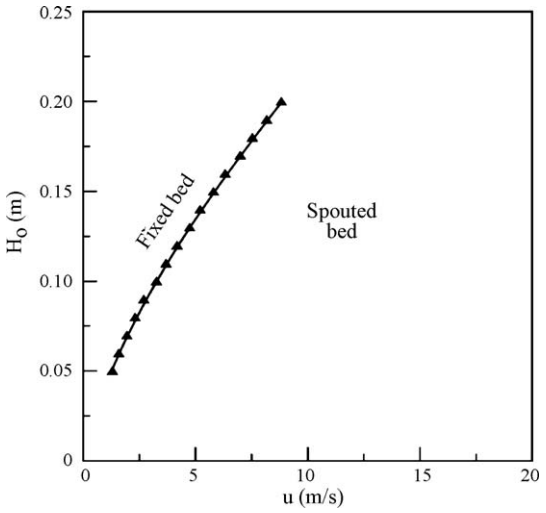

Fig. 6. Operation map for a silica gel of $\overline{d_S}$ 0.40 mm. Experimental system: $\gamma = 35^\circ$, $D_o = 0.006$ m.

Beginning in the fixed bed, increasing gas velocity the minimum spouting velocity is obtained. Furthermore, it is noticeable that this system is stable at all studied stagnant bed heights and that as stagnant bed height is increased minimum spouting velocity, increases, so the stable operation zone in spouted bed regime decreases.

In Fig. 7a, operation map for the contactor angle, 45°, in the same experimental conditions as in Fig. 6 has been plotted. As well as in the contactor of angle 35°, as stagnant bed height is increased,

Table 1
Properties of the solids.

Material	Particle diameter		Sauter average diameter $\overline{d_S}$ (10^{-3}) (m)	Density ρ_s (kg m^{-3})	Shape ϕ	Porosity ε_o	Geldart classification
	d_{p1} (10^{-3}) (m)	d_{p2} (10^{-3}) (m)					
Silica gel	0.16	0.30	0.21	910	0.87	0.48	A
	0.33	0.50	0.40	910	0.89	0.47	B
Pd/Al_2O_3	0.09	0.15	0.11	378	0.90	0.45	A
Y zeolite	0.08	0.10	0.09	1390	0.90	0.45	A

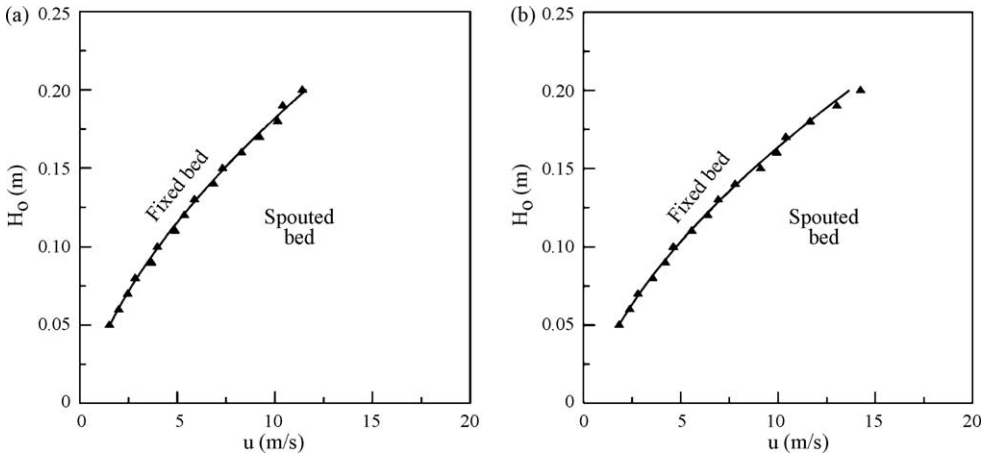

Fig. 7. Operation map for a binary mixture of silica gel of $\overline{d_S}$ 0.40 mm. Experimental system: $\gamma = 45^\circ$, (a) $D_o = 0.006$ m and (b) $D_o = 0.010$ m.

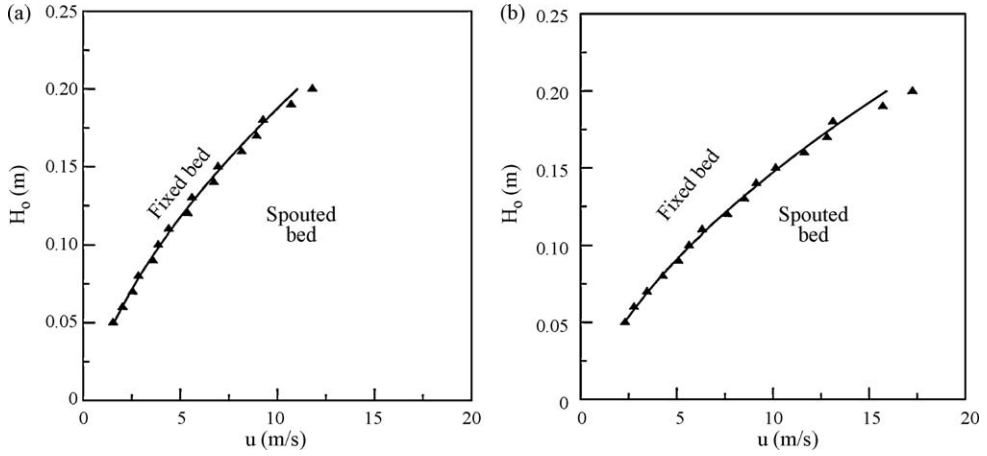

Fig. 8. Operation map for a silica gel of $\overline{d_S}$ 0.40 mm. Experimental system: $\gamma = 35^\circ$, $D_o = 0.006$ m, (a) at 150 °C and (b) at 350 °C.

air velocity increases. As it is observed, the increase in the contactor angle gives an increasing in air velocity.

The effect of the gas inlet diameter is observed comparing operating maps of Fig. 7a and b. As gas inlet diameter increases, the minimum spouting velocity necessary to reach the stable regime of spouting increases slightly.

The results in Fig. 8 correspond to the same experimental system as that in Fig. 6 at gas inlet temperatures of 150 and 350 °C. Comparing these figures, it is observed that as air inlet temperature increases, the minimum spouting velocity increases, so the stable operation zone decreases.

In Fig. 9 operation maps corresponding to beds made up of binary mixtures of Y zeolite of Sauter diameter $\overline{d_S} = 0.09$ mm, Fig. 9a, and of binary mixtures of Pd catalysts supported on Al_2O_3, of Sauter diameter $\overline{d_S} = 0.11$ mm, Fig. 9b, system of angle $\gamma = 35^\circ$, contactor gas inlet diameter, $D_o = 0.01$ m; at temperatures of 30 °C are shown.

As it is observed, the evolution for the bed consisting of Y zeolite passes from the fixed bed to an unstable regime, Fig. 9a.

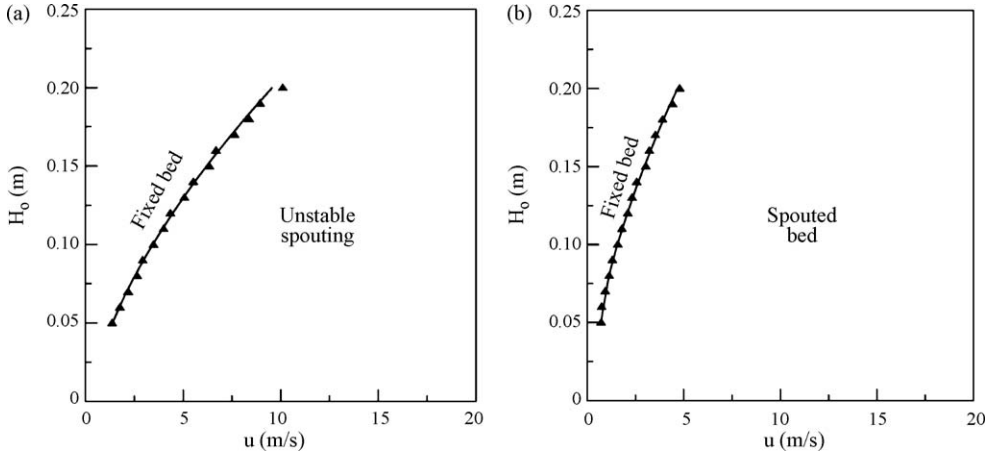

Fig. 9. Operation maps for experimental system: $\gamma = 35^\circ$, $D_o = 0.01$ m. (a) Y zeolite of $\overline{d_S}$ 0.09 mm and (b) Pd/Al_2O_3 of $\overline{d_S}$ 0.11 mm.

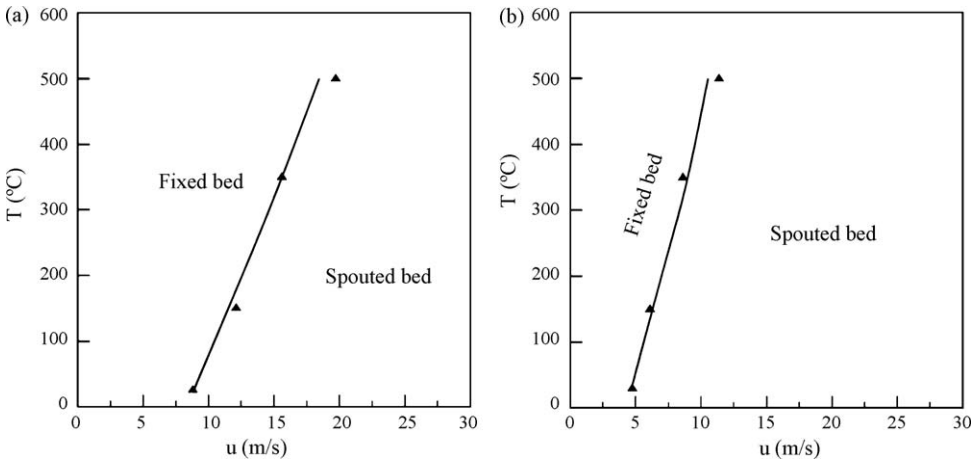

Fig. 10. Effect of the gas inlet temperature on the spouting regimes. Experimental system: γ = 35°; D_o = 0.006 m; H_o = 0.20 and binary mixtures of (a) silica gel of $\overline{d_S}$ = 0.4 mm and (b) Pd/Al_2O_3 of $\overline{d_S}$ = 0.11 mm.

Table 2
Experimental and calculated values of the minimum spouting velocity and relative error, for the different experimental systems.

Material	d_s (10^{-3}) (m)	ρ_s (kg m^{-3})	ϕ	γ (°)	D_o (m)	H_o (m)	T (°C)	$(u_{ms})_{exp}$ (m s^{-1})	$(u_{ms})_{cal}$ (m s^{-1})	% Relat. error
Silica gel	0.40	910	0.89	35	0.006	0.05	30	1.260	1.275	−1.19
	0.40	910	0.89	35	0.006	0.06	30	1.596	1.601	−0.31
	0.40	910	0.89	35	0.006	0.07	30	1.957	1.956	0.05
	0.40	910	0.89	35	0.006	0.08	30	2.328	2.339	−0.47
	0.40	910	0.89	35	0.006	0.09	30	2.701	2.749	−1.78
	0.40	910	0.89	35	0.006	0.10	30	3.277	3.186	2.77
	0.40	910	0.89	35	0.006	0.11	30	3.693	3.648	1.22
	0.40	910	0.89	35	0.006	0.12	30	4.170	4.135	0.84
	0.40	910	0.89	35	0.006	0.13	30	4.734	4.647	1.84
	0.40	910	0.89	35	0.006	0.14	30	5.191	5.183	0.15
	0.40	910	0.89	35	0.006	0.15	30	5.817	5.742	−1.29
	0.40	910	0.89	35	0.006	0.16	30	6.327	6.324	0.05
	0.40	910	0.89	35	0.006	0.17	30	7.003	6.929	1.06
	0.40	910	0.89	35	0.006	0.18	30	7.531	7.556	−0.33
	0.40	910	0.89	35	0.006	0.19	30	8.172	8.204	−0.39
	0.40	910	0.89	35	0.006	0.20	30	8.798	8.874	−0.86
Silica gel	0.40	910	0.89	45	0.006	0.05	30	1.521	1.540	−1.25
	0.40	910	0.89	45	0.006	0.06	30	2.001	1.962	1.95
	0.40	910	0.89	45	0.006	0.07	30	2.458	2.424	1.38
	0.40	910	0.89	45	0.006	0.08	30	2.835	2.926	−3.20
	0.40	910	0.89	45	0.006	0.09	30	3.684	3.464	5.97
	0.40	910	0.89	45	0.006	0.10	30	3.986	4.039	−1.33
	0.40	910	0.89	45	0.006	0.11	30	4.875	4.650	4.61
	0.40	910	0.89	45	0.006	0.12	30	5.352	5.294	1.08
	0.40	910	0.89	45	0.006	0.13	30	5.874	5.972	−1.67
	0.40	910	0.89	45	0.006	0.14	30	6.852	6.683	2.47
	0.40	910	0.89	45	0.006	0.15	30	7.315	7.425	−1.50
	0.40	910	0.89	45	0.006	0.16	30	8.285	8.199	1.04
	0.40	910	0.89	45	0.006	0.17	30	9.191	9.004	2.03
	0.40	910	0.89	45	0.006	0.18	30	10.138	9.839	2.95
	0.40	910	0.89	45	0.006	0.19	30	10.416	10.704	−2.76
	0.40	910	0.89	45	0.006	0.20	30	11.379	11.598	−1.92
Silica gel	0.40	910	0.89	45	0.010	0.05	30	1.832	1.813	1.04
	0.40	910	0.89	45	0.010	0.06	30	2.375	2.310	2.74
	0.40	910	0.89	45	0.010	0.07	30	2.784	2.855	−2.55
	0.40	910	0.89	45	0.010	0.08	30	3.561	3.445	3.26
	0.40	910	0.89	45	0.010	0.09	30	4.163	4.080	1.99
	0.40	910	0.89	45	0.010	0.10	30	4.629	4.757	−2.76
	0.40	910	0.89	45	0.010	0.11	30	5.568	5.475	1.67
	0.40	910	0.89	45	0.010	0.12	30	6.372	6.234	2.16
	0.40	910	0.89	45	0.010	0.13	30	6.921	7.033	−1.62
	0.40	910	0.89	45	0.010	0.14	30	7.790	7.869	−1.01
	0.40	910	0.89	45	0.010	0.15	30	9.112	8.744	4.04
	0.40	910	0.89	45	0.010	0.16	30	9.935	9.655	2.82
	0.40	910	0.89	45	0.010	0.17	30	10.400	10.603	−1.95
	0.40	910	0.89	45	0.010	0.18	30	11.641	11.586	0.47
	0.40	910	0.89	45	0.010	0.19	30	13.017	12.605	3.16
	0.40	910	0.89	45	0.010	0.20	30	14.235	13.657	4.06

Table 2 (*Continued*)

Material	d_s (10^{-3}) (m)	ρ_s (kg m^{-3})	ϕ	γ (°)	D_o (m)	H_o (m)	T (°C)	$(u_{ms})_{exp}$ (m s^{-1})	$(u_{ms})_{cal}$ (m s^{-1})	% Relat. error
Silica gel	0.40	910	0.89	35	0.006	0.05	150	1.541	1.586	−2.92
	0.40	910	0.89	35	0.006	0.06	150	2.019	1.990	1.43
	0.40	910	0.89	35	0.006	0.07	150	2.537	2.431	4.18
	0.40	910	0.89	35	0.006	0.08	150	2.851	2.907	−1.96
	0.40	910	0.89	35	0.006	0.09	150	3.584	3.417	4.66
	0.40	910	0.89	35	0.006	0.10	150	3.864	3.960	−2.48
	0.40	910	0.89	35	0.006	0.11	150	4.395	4.535	−3.18
	0.40	910	0.89	35	0.006	0.12	150	5.391	5.141	4.64
	0.40	910	0.89	35	0.006	0.13	150	5.583	5.777	−3.47
	0.40	910	0.89	35	0.006	0.14	150	6.720	6.443	4.12
	0.40	910	0.89	35	0.006	0.15	150	6.937	7.138	−2.90
	0.40	910	0.89	35	0.006	0.16	150	8.149	7.862	3.52
	0.40	910	0.89	35	0.006	0.17	150	8.915	8.613	3.39
	0.40	910	0.89	35	0.006	0.18	150	9.257	9.393	−1.47
	0.40	910	0.89	35	0.006	0.19	150	10.695	10.199	4.64
	0.40	910	0.89	35	0.006	0.20	150	11.815	11.032	6.63
Silica gel	0.40	910	0.89	35	0.006	0.05	350	2.318	2.287	1.34
	0.40	910	0.89	35	0.006	0.06	350	2.796	2.870	−2.65
	0.40	910	0.89	35	0.006	0.07	350	3.461	3.507	−1.33
	0.40	910	0.89	35	0.006	0.08	350	4.274	4.193	1.89
	0.40	910	0.89	35	0.006	0.09	350	5.091	4.929	3.18
	0.40	910	0.89	35	0.006	0.10	350	5.641	5.712	−1.26
	0.40	910	0.89	35	0.006	0.11	350	6.326	6.541	−3.40
	0.40	910	0.89	35	0.006	0.12	350	7.631	7.414	2.84
	0.40	910	0.89	35	0.006	0.13	350	8.517	8.332	2.17
	0.40	910	0.89	35	0.006	0.14	350	9.136	9.293	−1.72
	0.40	910	0.89	35	0.006	0.15	350	10.148	10.295	−1.45
	0.40	910	0.89	35	0.006	0.16	350	11.632	11.339	2.52
	0.40	910	0.89	35	0.006	0.17	350	12.814	12.423	3.05
	0.40	910	0.89	35	0.006	0.18	350	13.135	13.547	−3.13
	0.40	910	0.89	35	0.006	0.19	350	15.719	14.710	6.42
	0.40	910	0.89	35	0.006	0.20	350	17.257	15.911	7.80
Y zeolite	0.09	1390	0.90	35	0.006	0.05	30	1.358	1.375	−1.25
	0.09	1390	0.90	35	0.006	0.06	30	1.753	1.726	1.54
	0.09	1390	0.90	35	0.006	0.07	30	2.194	2.109	3.87
	0.09	1390	0.90	35	0.006	0.08	30	2.638	2.522	4.40
	0.09	1390	0.90	35	0.006	0.09	30	2.917	2.964	−1.61
	0.09	1390	0.90	35	0.006	0.10	30	3.474	3.435	1.12
	0.09	1390	0.90	35	0.006	0.11	30	4.018	3.933	2.11
	0.09	1390	0.90	35	0.006	0.12	30	4.342	4.459	−2.69
	0.09	1390	0.90	35	0.006	0.13	30	5.068	5.010	1.14
	0.09	1390	0.90	35	0.006	0.14	30	5.517	5.588	−1.28
	0.09	1390	0.90	35	0.006	0.15	30	6.351	6.191	2.52
	0.09	1390	0.90	35	0.006	0.16	30	6.674	6.818	−2.16
	0.09	1390	0.90	35	0.006	0.17	30	7.640	7.470	2.22
	0.09	1390	0.90	35	0.006	0.18	30	8.375	8.146	2.73
	0.09	1390	0.90	35	0.006	0.19	30	8.951	8.846	1.17
	0.09	1390	0.90	35	0.006	0.20	30	10.107	9.568	5.33
Pd/Al_2O_3	0.11	378	0.90	35	0.006	0.05	30	0.713	0.726	−1.82
	0.11	378	0.90	35	0.006	0.06	30	0.739	0.727	1.62
	0.11	378	0.90	35	0.006	0.07	30	0.928	0.912	1.72
	0.11	378	0.90	35	0.006	0.08	30	1.136	1.114	1.94
	0.11	378	0.90	35	0.006	0.09	30	1.294	1.332	−2.94
	0.11	378	0.90	35	0.006	0.10	30	1.587	1.566	1.32
	0.11	378	0.90	35	0.006	0.11	30	1.793	1.814	−1.17
	0.11	378	0.90	35	0.006	0.12	30	2.105	2.078	1.28
	0.11	378	0.90	35	0.006	0.13	30	2.316	2.355	−1.68
	0.11	378	0.90	35	0.006	0.14	30	2.574	2.647	−2.83
	0.11	378	0.90	35	0.006	0.15	30	3.031	2.952	2.61
	0.11	378	0.90	35	0.006	0.16	30	3.216	3.271	−1.71
	0.11	378	0.90	35	0.006	0.17	30	3.527	3.602	−2.12
	0.11	378	0.90	35	0.006	0.18	30	3.895	3.947	−1.33
	0.11	378	0.90	35	0.006	0.19	30	4.413	4.304	2.47
	0.11	378	0.90	35	0.006	0.20	30	4.786	4.673	2.36
Silica gel	0.40	910	0.89	35	0.006	0.20	30	8.798	8.874	−0.86
	0.40	910	0.89	35	0.006	0.20	150	11.815	11.032	6.63
	0.40	910	0.89	35	0.006	0.20	350	17.257	15.911	7.79
	0.40	910	0.89	35	0.006	0.20	500	19.714	18.461	6.36
Pd/Al_2O_3	0.11	378	0.90	35	0.006	0.20	30	4.786	4.673	2.36
	0.11	378	0.90	35	0.006	0.20	150	6.152	6.284	−2.14
	0.11	378	0.90	35	0.006	0.20	350	8.617	9.072	−5.28
	0.11	378	0.90	35	0.006	0.20	500	11.375	10.526	7.46

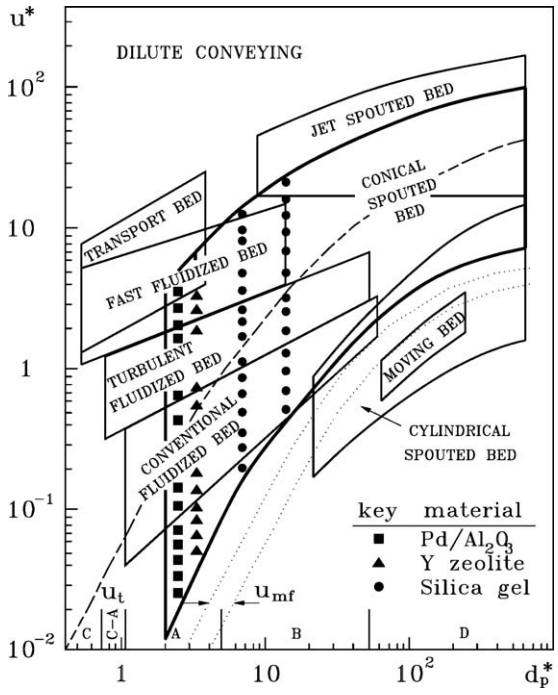

Fig. 11. Applicability ranges of the regimes in conical spouted beds and other methods for gas–solid contact.

Nevertheless, the bed consisting of binary mixtures of Pd catalysts supported on Al_2O_3, Fig. 9b, is stable for all the stagnant bed heights studied and, minimum spouting velocity increases as stagnant bed height is increased.

The operation map corresponding to beds consisting of Pd catalysts supported on Al_2O_3, of Sauter diameter $\overline{d_S} = 0.11$ mm, system of angle $\gamma = 35°$, contactor gas inlet diameter, $D_o = 0.006$ m; at temperatures of 30 °C is shown in Fig. 10. As it is observed, the system is stable for all the stagnant bed heights studied and, minimum spouting velocity increases as stagnant bed height is increased.

In Fig. 10 the spouting regimes for different velocities and gas inlet temperatures in plots of gas inlet diameter, T, against gas velocity, u are shown for silica gel of Sauter average diameter $\overline{d_S}$ 0.4 mm, Fig. 10a, and for Pd catalysts supported on Al_2O_3, of Sauter average diameter $\overline{d_S}$ 0.11 mm, Fig. 10b.

As it is observed, starting from the fixed bed, stable spouted bed regime existed for all the experimental systems studied. As gas inlet temperature increases, the gas velocity to reach the spouted bed regime increases, so the spouted bed zone decreases.

3.3. Minimum spouting velocity

The validity of the correlation already proposed for calculation of the minimum spouting velocity at room temperatures with uniform beds consisting of fine particles [24] has been proven with beds made up of catalyst at a range of temperatures between 25 and 500 °C.

$$(Re_{ms})_o = 0.126 Ar^{0.39} \left(\frac{D_b}{D_o}\right)^{1.68} \tan(\gamma/2)^{-0.57} \quad (1)$$

The regression coefficient of minimum spouting velocity of all the experimental data is $r^2 = 0.984$ and the maximum relative error is below ±8%. The good agreement of the experimental values (points) to the calculated ones (lines) in Figs. 6–10 verified the validity of the equation of spouted bed. The experimental values and the values calculated with Eq. (1) of the minimum spouting velocity in beds consisting of catalyst, represented in Figs. 6–10, for different geometric factors and experimental conditions, are summarized in Table 2.

3.4. Comparison with other gas–solid contact regimes

The experimental applicability ranges of the different regimes in conical spouted bed are compared in Fig. 11, in which the application conditions of other methods for gas–solid contact, in a map of velocity modulus $u^* = u[\rho^2/\Delta\rho g\mu]^{1/3}$ vs. the modulus related to particle size-density, $d_p^* = Ar^{1/3}$ are shown for catalyst of different particle diameter and density.

The ranges corresponding to the Geldart classification [27,28] have been expressed on the abscissa axis of Fig. 11. The calculated terminal velocity curve, u_t, has been drawn with a stroke line. The values of minimum fluidization velocity, u_{mf}, have been drawn with a dotted line. They are within a range, as the value calculated would vary according to the correlation used.

The experimental values (points) for beds made up of catalyst of different particle diameter have been plotted. The conical spouted beds cover a very wide range of application conditions, fluidized beds, turbulent fluidized beds and transport bed and fast fluidized bed and part of the conditions of other contact regimes like cylindrical spouted beds and jet spouted beds. In this figure, the velocity is referred to the upper diameter corresponding to the stagnant bed height, D_b.

4. Conclusions

In order to determine the stable operating conditions and the applicability of this method in spouted bed regime for the thermal catalytic treatment of wastes in order to environmental improvement, a hydrodynamic study has been carried out with beds consisting of binary mixtures of catalyst.

Beginning in the fixed bed, as gas velocity is increased the stable regime of spouted bed is reached. Minimum spouting velocity increases as stagnant bed height, contactor angle, gas inlet diameter and gas inlet temperature are increased, therefore operating zone in stable spouted bed regime decreases.

The correlation already proposed for calculation of the minimum spouting velocity for beds consisting of fine particles, at room temperatures [23] is valid for stable operation in these contactors with uniform beds of catalyst of different particle diameter and density and in a wide range of operating conditions at temperatures above room temperature (at a temperature range of 25–500 °C).

The conical spouted beds cover a very wide range of application conditions, fluidized beds, turbulent fluidized beds and transport bed and fast fluidized bed and part of the conditions of other contact regimes like cylindrical spouted beds and jet spouted bed.

Therefore, the results of hydrodynamic conditions in the handling of catalyst particles have determined that the spouted bed in exclusively conical contactors allows for operating with catalyst in stable regime and without noticeable segregation, so this contact regime has good prospects for its use in operations and processes that require handling of fine particles.

Acknowledgments

This work was carried out with the financial support of the University and of the County Council of Biscay (Project DIPE 07/09).

References

[1] R.K. Konduri, E.R. Altwicker, M.H. Morgan III, Chem. Eng. Sci. 54 (2) (1999) 185.
[2] M.G. Rasul, Fuel 80 (15) (2001) 2189.
[3] M.J. San José, R. Aguado, S. Alvarez, M. Olazar, Información Tecnol. 13 (2) (2002) 127.

[4] M.J. San José, A. Ortíz de Salazar, S. Alvarez, M. Olazar, Información Tecnol. 13 (2) (2002) 133.
[5] M.J. San José, S. Alvarez, A. Ortiz de Salazar, M. Olazar, J. Bilbao, Science in Thermal and Chemical Biomass Conversion, 1, CPL press, Newbury Berks, 2006, pp. 228.
[6] S. Hanson, J.W. Patrick, A. Walker, Fuel 81 (5) (2002) 531.
[7] A. Adegoroye, N. Paterson, X. Li, T. Morgan, A.A. Herod, D.R. Dugwell, R. Kandiyoti, Fuel 83 (2004) (1949).
[8] P.A. Salam, S.C. Bhattacharya, Energy 31 (2006) 228.
[9] A. Mendes, A. Dollet, C. Ablitzer, C. Perrais, G. Flamant, J. Anal. Appl. Pyrolysis 82 (1) (2008) 117.
[10] A. Jarallah, A.P. Watkinson, Can. J. Chem. Eng. 63 (2) (1985) 227.
[11] R. Aguado, M. Olazar, M.J. San José, G. Aguirre, J. Bilbao, Ind. Eng. Chem. Res. 39 (6) (2000) 1925.
[12] M. Olazar, R. Aguado, M.J. San José, J. Bilbao, J. Chem. Technol. Biotechnol. 76 (5) (2001) 469.
[13] Y. Uemura, M. Azeura, Y. Ohzuno, Y. Hatate, J. Chem. Eng. Jpn. 34 (10) (2001) 1293.
[14] R. Aguado, M. Olazar, M.J. San José, B. Gaisan, J. Bilbao, Energy Fuels 16 (6) (2002) 1429.
[15] R. Aguado, M. Olazar, S. Alvarez, P. González, J. Bilbao, Pyrolysis and Gasification of Biomass and Wastes Expert Meeting, vol. 4, CPL Press, Newbury, Gran Bretaña, 2003, p. 41.
[16] R. Aguado, R. Prieto, M.J. San José, M. Olazar, S. Alvarez, J. Bilbao, Chem. Eng. Process. 44 (2005) 231.
[17] M. Olazar, R. Aguado, M.J. San José, S. Alvarez, J. Bilbao, Powder Technol. 165 (3) (2006) 128.
[18] W. Zhu, W. Song, W. Lin, Energy Fuels 22 (4) (2008) 2482.
[19] M. Olazar, M.J. San José, A.T. Aguayo, J.M. Arandes, J. Bilbao, Ind. Eng. Chem. Res. 31 (7) (1992) 1784.
[20] M. Olazar, M.J. San José, F.J. Peñas, A.T. Aguayo, J. Bilbao, Ind. Eng. Chem. Res. 32 (1993) 2826.
[21] M.J. San José, M. Olazar, F.J. Peñas, J. Bilbao, Ind. Eng. Chem. Res. 33 (1994) 1838.
[22] M.S. Bacelos, J.T. Freire, Ind. Eng. Chem. Res. 45 (2006) 808.
[23] M. Olazar, M.J. San José, G. Zabala, J. Bilbao, Chem. Eng. Sci. 49 (1994) 4579.
[24] M. Olazar, M.J. San José, E. Cepeda, R. Ortiz de Latierro, J. Bilbao, Fluidization VIII, 1995, p. 197.
[25] M. Olazar, M.J. San José, S. Alvarez, A. Morales, J. Bilbao, Ind. Eng. Chem. Res. 43 (2004) 655.
[26] M.J. San José, M. Olazar, S. Alvarez, A. Morales, J. Bilbao, Ind. Eng. Chem. Res. 44 (2005) 193.
[27] D. Geldart, Powder Technol. 7 (5) (1973) 285.
[28] D. Geldart, Gas Fluidization Technology, John Wiley, New York, 1986.
[29] K.B. Mathur, P.E. Gishler, AIChE J. 1 (1955) 157.